

Polarization response of proton irradiated 0.9Pb(Mg_{1/3}Nb_{2/3})O₃-0.1PbTiO₃/polyvinylidene fluoride-trifluoroethylene 0-3 composites

K. H. Lam and H. L. W. Chan

Department of Applied Physics and Materials Research Centre, The Hong Kong Polytechnic University, Hungghom, Kowloon, Hong Kong, China

(Received 22 March 2004; accepted 9 August 2004)

Polyvinylidene fluoride-trifluoroethylene [P(VDF-TrFE) 70/30 mol %] copolymer can be transformed from a normal ferroelectric to a relaxor ferroelectric material after proton irradiation. The phase transition peak broadens and shifts towards lower temperature as the measurement frequency decreases. The occurrence of a slim polarization-electric field loop is another evidence of the effect of proton irradiation. In the present study, 0-3 composites are fabricated by incorporating 0.9Pb(Mg_{1/3}Nb_{2/3})O₃-0.1PbTiO₃ ceramic powder into a P(VDF-TrFE) 70/30 mol % copolymer matrix. 0.9PMN-0.1PT ceramic is a relaxor ferroelectric with high dielectric permittivity. It was found that the relative permittivity of an unirradiated PMN-PT/P(VDF-TrFE) 0-3 composite increases with increasing ceramic volume fraction. With a dosage of 1000 kGy (where 1 Gy = 100 rad), the composite exhibits a broad peak in the relative permittivity. In the unirradiated composites, the remnant polarization increases gradually with PMN-PT volume fraction. After irradiation, the remnant polarization of the composites with different PMN-PT volume fractions is similar to that of the irradiated copolymer. Energy storage capabilities of the samples were evaluated which showed that proton irradiated composites have a potential for energy storage applications. © 2004 American Institute of Physics. [DOI: 10.1063/1.1803631]

I. INTRODUCTION

Piezoelectric ceramic/polymer composites have the compliance of polymers which overcome the problems of brittleness in piezoceramics. By imbedding piezoelectric ceramic powder into a polymer matrix, 0-3 composites with good mechanical properties and high dielectric breakdown strength can be developed. These composites can be used in capacitor and energy storage devices.^{1,2}

Since the relative permittivity ϵ of 0-3 composites are dominated by the polymer matrix, the resulting 0-3 composites also have low ϵ compared with the ceramics. In order to improve the energy storage capability, the relative permittivity of this type of composite should be increased. Hence, different ceramics and polymer matrices have been used in the past to optimize ϵ .³⁻⁵ 0.9Pb(Mg_{1/3}Nb_{2/3})O₃-0.1PbTiO₃ (0.9PMN-0.1PT) is a lead-based relaxor material with very high dielectric permittivity near room temperature⁶ and it also has a low remnant polarization. In this work, polyvinylidene fluoride-trifluoroethylene [P(VDF-TrFE)] ferroelectric copolymer is used as the polymer matrix because it has high ϵ compared to other polymers.⁷ Besides using different materials, irradiation was also used to improve the dielectric properties of the composites. It was found that the dielectric properties of P(VDF-TrFE) copolymer can be changed significantly after irradiation.^{8,9} When the irradiated copolymer was used as the matrix, the resulting composites have higher relative permittivity which improves their charge storage capability.^{10,11}

In this work, 0.9PMN-0.1PT and P(VDF-TrFE) 70/30 mol % were used as the ceramic inclusion and poly-

mer matrix, respectively. The 0-3 composites were subjected to high-energy proton irradiation. Properties of the composites, including the dielectric behavior and polarization response, and their variations with ceramic volume fraction and irradiation dosage were investigated.

II. EXPERIMENT

0.9PMN-0.1PT ceramic powder was fabricated using the Columbite method.¹² First, magnesium oxide and niobium pentoxide were prereacted at 1100 °C to form magnesium niobate. After the prereaction, the magnesium niobate was reacted with lead oxide and titanium oxide to give PMN-PT. This method suppressed the growth of the pyrochlore phase and thus produced PMN-PT ceramic powder with a pure perovskite phase. The powder was calcinated at 850 °C and sintered at 1200 °C for 2 h. In order to reduce the particle size, the powder was ball milled in ethanol for 10 h. The P(VDF-TrFE) 70/30 mol % copolymer powder was supplied by Piezotech Co., St. Louis, France.

0-3 composites were prepared by solvent casting. The copolymer powder was dissolved in methylethylketone and then the ceramic powder was added. Ultrasonic agitation was used to disperse the powder. The mixture was continuously stirred at 60 °C during evaporation of solvent until the composite was almost dry. Then, the composite was dried at 80 °C in an oven overnight to ensure the complete evaporation of solvent and moisture.

The bulk composites were fabricated by hot pressing. The dried composite was cut into small pieces and then compression-molded at 230 °C into composite film with a

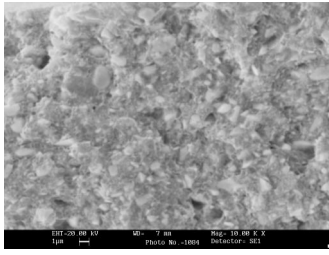


FIG. 1. Scanning electron microscopy micrograph of a 0.9PMN-0.1PT/P(VDF-TrFE) 0-3 composite with 0.3 ceramic volume fraction.

thickness of $\sim 30 \mu\text{m}$. Composites with ceramic volume fractions ranging from 0.05 to 0.40 were fabricated. The bulk composites were annealed under pressure at 120°C for 2 h.

Proton (H^+ ions) irradiation was carried out in an accelerator (High Voltage Engineering) located at the Chinese University of Hong Kong. The energy of protons should be high enough to go through the composites so that the microstructure of the whole composite film can be modified but no protons were implanted in the polymer. The samples were irradiated by 3 MeV protons at ambient temperature in vacuum. During the irradiation process, a low beam current at a level of $\sim 3.8 \text{ nA}$ was used to prevent excessive temperature elevation in the films. The fluence rate (number of proton ions injected per unit area of the target material per second) was $\sim 6.24 \times 10^{13} \text{ ions/m}^2/\text{s}$. The irradiation dosages were chosen for maximizing the relative permittivity of the composites near room temperature. Three dosages, $3.57 \times 10^{17} \text{ ions/m}^2$ (600 kGy), $4.76 \times 10^{17} \text{ ions/m}^2$ (800 kGy), and $5.96 \times 10^{17} \text{ ions/m}^2$ (1000 kGy) were used. The samples were then electroded with chromium gold by evaporation for further measurements. After electroding, the samples should be annealed under pressure at 120°C for 2 h to improve the adhesion between the electrode and the composite. The dielectric properties of the samples were measured as a function of temperature using an HP4194A impedance/gain phase analyzer. The polarization-electric field (P - E) hysteresis loop measurements were carried out using a modified Sawyer Tower circuit at a frequency of 10 Hz.

III. RESULTS AND DISCUSSION

The distribution of ceramic powder inside the composites is revealed by using scanning electron microscopy (Leica stereo scan 440). Figure 1 shows that cross-sectional view of a composite with 0.3 ceramic volume fraction. It is seen that the powder is uniformly distributed throughout the copolymer matrix and the average particle size is around $1 \mu\text{m}$.

Before proton irradiation, dielectric properties of the composites were characterized. The relative permittivity and loss tangent ($\tan \delta$) of the composites were measured at 1 kHz at room temperature as a function of the ceramic volume fraction as shown in Figure 2. The relative permittivity and dielectric loss increase with the ceramic volume fraction. It was found that the experimental data agree quite well with the Bruggeman model,¹³

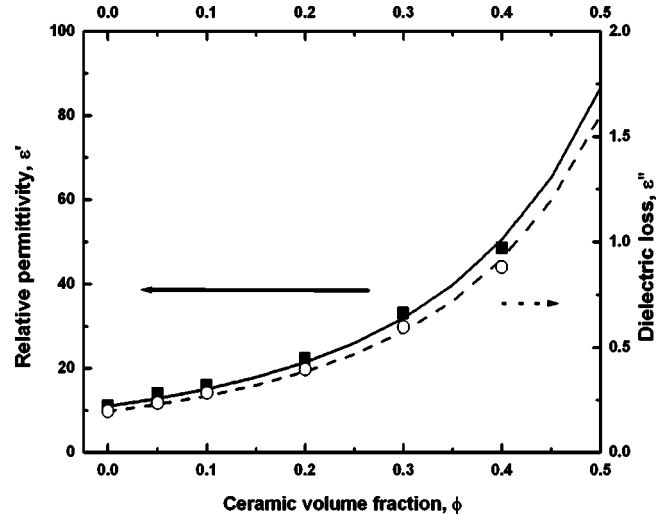


FIG. 2. Dielectric properties (1 kHz) of the unirradiated unpoled composites at 25°C as a function of PMN-PT volume fraction. The solid curve (ϵ') and dashed curve (ϵ'') are calculated from the Bruggeman model. Solid squares and hollow circles are the experimental data.

$$\frac{\epsilon'_c - \epsilon'}{(\epsilon')^{1/3}} = \frac{(1 - \phi)(\epsilon'_c - \epsilon'_p)}{(\epsilon'_p)^{1/3}}, \tag{1}$$

$$\epsilon'' = \frac{(\epsilon'_c - \epsilon')(\epsilon'_c + 2\epsilon'_p)\epsilon''}{(\epsilon'_c - \epsilon'_p)(\epsilon'_c + 2\epsilon')\epsilon'_p} + \frac{3(\epsilon' - \epsilon'_p)\epsilon''}{(\epsilon'_c - \epsilon'_p)(\epsilon'_c + 2\epsilon')}\epsilon''_c, \tag{2}$$

where ϕ is the ceramic volume fraction of the composite. ϵ' and $\epsilon''(=\epsilon' \tan \delta)$, ϵ'_c and $\epsilon''_c(=\epsilon'_c \tan \delta_c)$, ϵ'_p and $\epsilon''_p(=\epsilon'_p \tan \delta_p)$ are the relative permittivity and dielectric loss of the composite, ceramic inclusion, and polymer matrix, respectively. In the theoretical calculation, the relative permittivity and loss tangent of the unpoled copolymer ($\epsilon'_p = 11; \tan \delta_p = 0.018$) and sintered ceramics ($\epsilon'_c = 15000; \tan \delta_c = 0.065$) were measured at room temperature at 1 kHz. It is found that the experimental data of the unpoled composites agree quite well with the theoretical calculation.

Figure 3 shows the relative permittivity (1 kHz) of the composite with 0.3 ceramic volume fraction as a function of temperature after different irradiation dosages. In the unirradiated composite, the phase transition peak occurs at about 110°C upon heating and at about 75°C upon cooling, showing a thermal hysteresis effect.¹⁴ Since this effect represents a typical first-order phase transition in the copolymer, the peaks in ϵ for the composite originate from the copolymer matrix. As shown in the figure, broader permittivity peaks and higher room-temperature relative permittivity ϵ are obtained after irradiation. Since the peaks move towards lower temperatures, ϵ at room temperature increases significantly. ϵ of the irradiated composites have little or no thermal hysteresis during the heating and cooling process. It indicates that the composites are no longer a normal ferroelectric after irradiation. Besides, the relative permittivity and temperature dependence can be varied by using different irradiation dosages. Among the three irradiation dosages, it is found that a proton dosage of 4.76

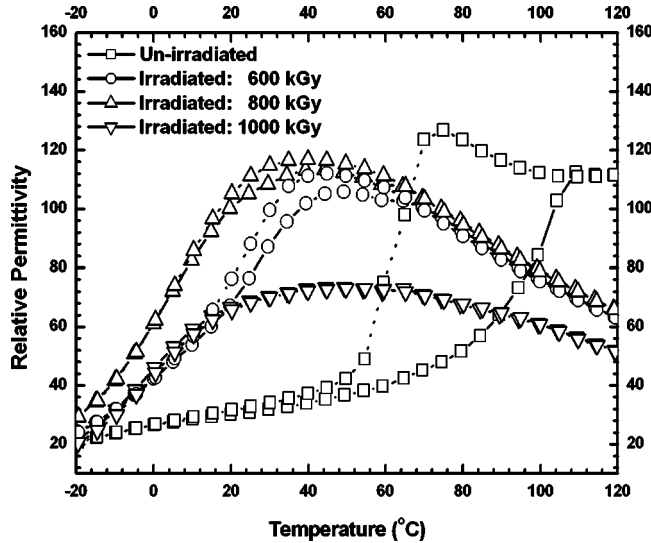


FIG. 3. Temperature dependence of the relative permittivity (1 kHz) of composites with 0.3 PMN-PT volume fraction with different irradiation dosages. [Solid line, heating process; dotted line, cooling process].

$\times 10^{17}$ ions/m² (800 kGy) can maximize the relative permittivity of the composites near room temperature.

Figure 4 shows the temperature and frequency dependence of the permittivity and dielectric loss of the irradiated (800 kGy) composite with 0.4 ceramic volume fraction. Both peaks of the relative permittivity and loss tangent move towards higher temperature with increasing measurement frequency. This broad diffuse and frequency dependent transition peak is a major characteristic of relaxor ferroelectrics.^{15,16} The relative permittivity of the composite is as high as 140 (at 1 kHz) at room temperature.

The electric displacement-electric field hysteresis loops of the unirradiated and irradiated PMN-PT/P(VDF-TrFE) 0-3 composites with 0.3 ceramic volume fraction are shown in Figure 5. The unirradiated composite exhibits a typical ferroelectric hysteresis loop. For the irradiated composites, the

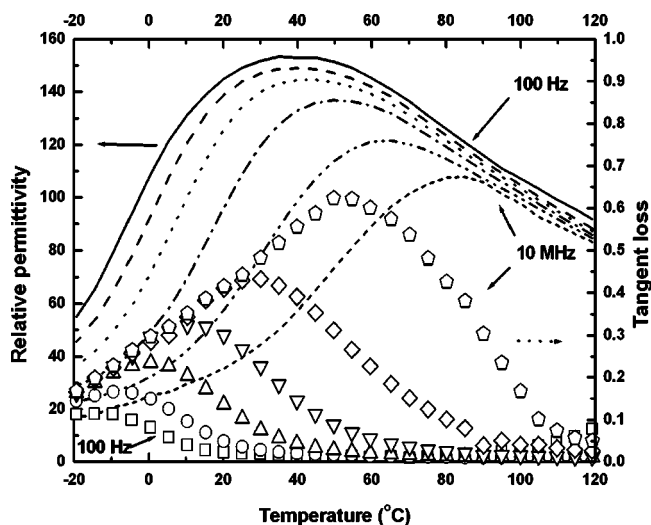


FIG. 4. Temperature dependence of the relative permittivity and tangent loss of irradiated composites (dosage: 800 kGy) with 0.4 ceramic volume fraction are plotted at different frequencies (100 Hz, 1 kHz, 10 kHz, 100 kHz, 1 MHz) [Line, relative permittivity; symbols, tangent loss].

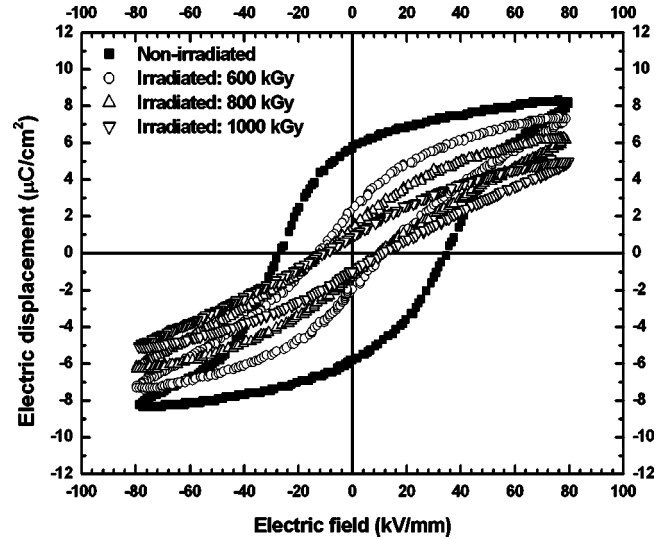


FIG. 5. Hysteresis loops of the irradiated composites ($\phi=0.3$) with different irradiation dosages.

hysteresis loops become slimmer. The proton irradiation breaks up the coherent polarization domains into nanopolar regions, resulting in converting the normal ferroelectric material to a relaxor ferroelectric.¹⁷ With increase in the irradiation dosage, the polarization level reduces gradually while the coercive field remains constant.

The hysteresis loops of the pure copolymer and composites before and after irradiation (800 kGy) are shown in Figures 6(a) and 6(b), respectively. For the unirradiated samples, the remnant polarization increases and the coercive field decreases as ϕ increases. After irradiation, the hysteresis loop of both the pure copolymer and the 0-3 composites become slimmer. It is noted that the size of their hysteresis loops is similar such that the remnant polarization and the coercive field of the irradiated composites are comparable to that of the irradiated copolymer. The coercive field and remnant polarization of the samples before and after irradiation (800 kGy) are summarized as a function of PMN-PT volume fraction in Fig. 7. Both the coercive field and remnant polarization of the irradiated composites even with 0.4 ceramic volume fraction exhibit a drastic drop, reaching the levels of irradiated copolymer. The values seem to be independent of the ceramic volume fraction. The dependence of the remnant polarization and coercive field on the ceramic volume fraction is quite different from the phenomenon observed by Adikary *et al.*¹⁸ which used the normal ferroelectric BST powder as the inclusion in the 0-3 composites. In their work, after irradiation, the contribution of the BST ceramic phase is clearer as the ceramic volume fraction increases. In the present study, the ceramic inclusion used is a relaxor ferroelectric 0.9PMN-0.1PT ceramic powder which is not subjected to conversion from ferroelectric to relaxor phase upon proton irradiation. The ferroelectric properties of the irradiated composites, even after increasing the content of the relaxor ceramic phase, are comparable to that of the irradiated copolymer.

For electrical energy storage application, the stored energy density is an important parameter in a linear dielectric

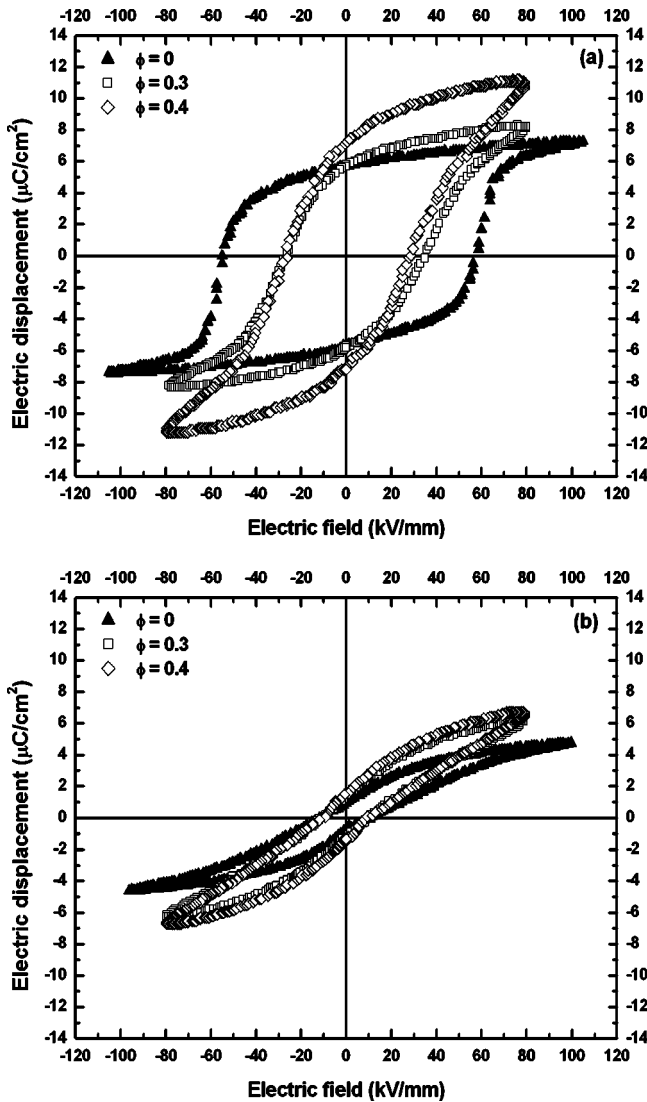


FIG. 6. Hysteresis loops of the copolymer and composites with different PMN-PT volume fraction ϕ . (a) Before irradiation. (b) After irradiated at a dosage of 800 kGy.

material. Since ferroelectric materials have nonlinear dielectric properties, the density of energy stored in a nonlinear dielectric material J is given by

$$J = \int_0^{D_{\max}} EdD, \tag{3}$$

where E is the electric field, D the electric displacement, ϵ_0 and ϵ_r are the permittivity of vacuum and relative permittivity, respectively.¹⁹ Based on the equation, the energy storage of a dielectric system mainly depends on the electrical breakdown strength and the relative permittivity. Figure 8 shows a typical D - E hysteresis loop in a normal ferroelectric material and the shaded area represents the energy per unit volume available upon discharge.²⁰ Figure 9 shows the energy storage of the unirradiated and irradiated composites as a function of ϕ , which was quantitatively determined (under an electric field of 80 kV/mm) from the D - E loops shown in Fig. 6. It is seen that, for both unirradiated and irradiated samples, the energy storage increases with the ceramic vol-

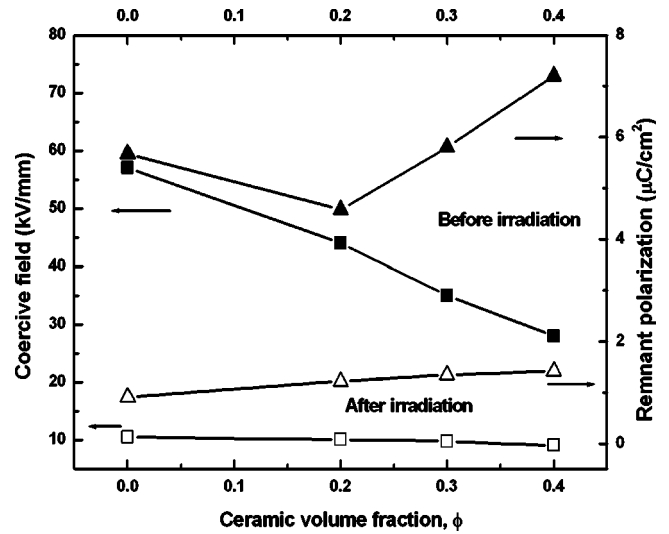


FIG. 7. Coercive field and remnant polarization of composites as a function of PMN-PT volume fraction ϕ . Solid and hollow symbols denote data before irradiation and after irradiation at a dosage of 800 kGy, respectively.

ume fraction. By comparing the D - E loops of the copolymer and composites, it can be seen that the loops become slimmer with increasing ϕ so that the energy storage increases with ϕ . Similarly, irradiated composites show higher energy storage than that of unirradiated composites because the hysteresis loops of the composites are also slimmer after irradiation. For unirradiated composites with low ϕ , there is not much difference of energy storage compared with the copolymer until ϕ is greater than 0.2. Since the energy storage of the unirradiated composites mainly contributed by the high dielectric ceramic inclusion, an almost linear increase in energy storage with ϕ can be seen. In the irradiated composites, a steep increase in energy storage can be observed even when ϕ is low ($\phi=0.2$). The energy storage capability of the irradiated composites is not only contributed by the relaxor ceramic inclusions, but also by the relaxorlike polymer matrix. When comparing the different proton dosages, the energy storage of the samples increases with the dosage. The energy storage of the irradiated composites is much higher than that of nonpolar polymer/antiferroelectric ceramics

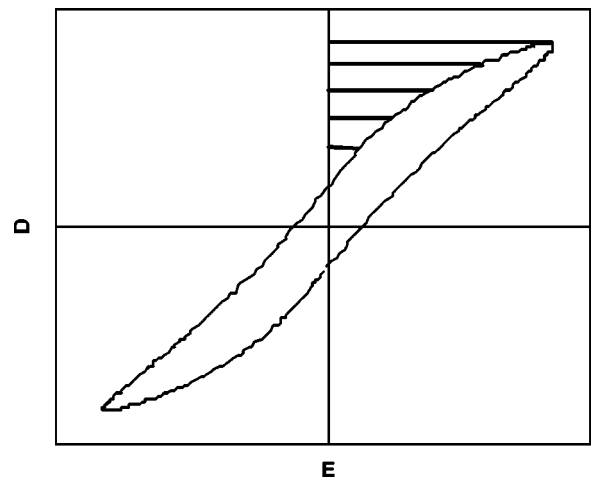


FIG. 8. D - E hysteresis loop and energy storage in a normal ferroelectric material. The shaded area denotes the discharge energy.

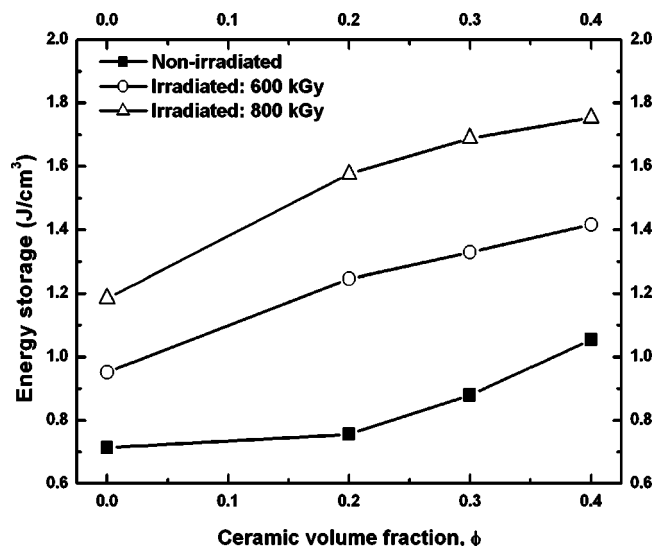


FIG. 9. Energy storage as a function of ceramic volume fraction for unirradiated and irradiated (600 kGy and 800 kGy) composites.

composites and comparable to that of the multilayer ceramic capacitors reported in the literatures.^{21,22}

IV. CONCLUSION

The dielectric properties and polarization response of proton irradiated 0.9PMN-0.1PT/P(VDF-TrFE) 0-3 composites have been studied. With the combination of two high relative permittivity phases, the dielectric properties of the composites can be improved significantly. After irradiation, the dielectric peak broadens and the transition temperature shifts to a lower temperature (from 75 °C to 35 °C). With an irradiation dosage of 800 kGy, the room temperature relative permittivity of a 0-3 composite with 0.4 ceramic volume fraction is 140. Both the coercive field and remnant polarization of the irradiated composites drop substantially to the level similar to that of the irradiated copolymer. The energy storage capability of the composites is significantly increased after irradiation.

ACKNOWLEDGMENTS

This work was supported by the Hong Kong Research Grants Council Grant No. (RGC PolyU-5147/02E) and the Centre for Smart Materials of the Hong Kong Polytechnic University. Thanks are also due to Professor I. H. Wilson and Dr. E. Z. Luo of the Chinese University of Hong Kong for their help in proton irradiation of P(VDF-TrFE) copolymers.

¹Y. Rao, S. Ogitani, P. Kohl, and C. P. Wong, International Symposium on Advanced Packing Materials, 2000, p. 32.

²G. Randolph, H. Fraiss-Kolbl, and H. Hauser, IEEE Annual Report **1**, 220 (1996).

³C. J. Dias and D. K. Das-Gupta, Proceedings of the Fourth International Conference on Properties and Applications of Dielectric Materials, 1994, p. 4101.

⁴Q. Q. Zhang, H. L. W. Chan, and C. L. Choy, Composites, Part A **30**, 163 (1998).

⁵Y. Chen, H. L. W. Chan, and C. L. Choy, IEEE Proceedings on Applications of Ferroelectrics, 1996, Vol. 2, p. 619.

⁶M. Villegas, A. C. Caballero, M. Kosec, C. Moure, P. Duran, and J. F. Fernandez, J. Mater. Res. **14**, 891 (1999).

⁷T. Furukawa, J. X. Wen, K. Suzuki, Y. Takashina, and M. Date, J. Appl. Phys. **56**, 829 (1984).

⁸Q. M. Zhang, Z. Y. Cheng, and V. Bharti, J. Appl. Phys. **70**, 307 (2000).

⁹Q. M. Zhang, V. Bharathi, and X. Zhao, Science **280**, 2101 (1998).

¹⁰Y. Bai, Z. Y. Cheng, V. Bharti, H. S. Xu, and Q. M. Zhang, IEEE Proceedings on Applications of Ferroelectrics, 2000, Vol. 2, p. 797.

¹¹S. U. Adikary, H. L. W. Chan, C. L. Choy, B. Sundarvel, and I. H. Wilson, Compos. Sci. Technol. **62**, 2161 (2002).

¹²S. L. Swartz and T. R. Shrout, Mater. Res. Bull. **17**, 1245 (1982).

¹³D. A. G. Bruggeman, Ann. Phys. (Leipzig) **24**, 635 (1935).

¹⁴T. Furukawa, *Key Engineering Materials*, edited by D. K. Das-Gupta (Trans Tech, Switzerland, 1994), Vol. 92-94, pp. 20-23, Chap. 7.

¹⁵T. R. Shrout and J. Fielding, Jr, IEEE Proceedings on Ultrasonics, 1990, Vol. 2, p. 711.

¹⁶L. E. Cross, Ferroelectrics **76**, 241 (1987).

¹⁷S. T. Lau, H. L. W. Chan, B. Sundarvel, I. H. Wilson, and C. L. Choy, 111th International Symposium on Electrets, 2002, p. 102.

¹⁸S. U. Adikary, H. L. W. Chan, C. L. Choy, B. Sundarvel, and I. H. Wilson, Jpn. J. Appl. Phys., Part 1 **41**, 6938 (2002).

¹⁹I. Burn and D. M. Smyth, J. Mater. Sci. **7**, 339 (1972).

²⁰B. Jaffe, Proc. IRE **49**, 1264 (1961).

²¹D. K. Das-Gupta and S. Zhang, Ferroelectrics **134**, 71 (1992).

²²G. R. Love, J. Am. Ceram. Soc. **73**, 323 (1990).